On the interference of ggH and c̄cH Higgs production mechanisms and the determination of charm Yukawa coupling at the LHC

Wojciech Bizoń,[a,b] **Kirill Melnikov**[a] **and Jérémie Quarroz**[a]

[a]*Institute for Theoretical Particle Physics (TTP), Karslruhe Institute of Technology,*
Wolfgang-Gaede Straße 1, Karlsrue D-76128, Germany

[b]*Institute for Astroparticle Physics (IAP), Karslruhe Institute of Technology,*
Hermann-von-Helmholtz-Platz 1, Eggenstein-Leopoldshafen D-76344, Germany

E-mail: wojciech.bizon@kit.edu, kirill.melnikov@kit.edu,
jeremie.quarroz@kit.edu

ABSTRACT: Higgs boson production in association with a charm-quark jet proceeds through two different mechanisms — one that involves the charm Yukawa coupling and the other that involves direct Higgs coupling to gluons. The interference of the two contributions requires a helicity flip and, therefore, cannot be computed with massless charm quarks. In this paper, we consider QCD corrections to the interference contribution starting from charm-gluon collisions with massive charm quarks and taking the massless limit, $m_c \to 0$. The behavior of QCD cross sections in that limit differs from expectations based on the canonical QCD factorization. This implies that QCD corrections to the interference term necessarily involve logarithms of the ratio M_H/m_c whose resummation is currently unknown. Although the explicit next-to-leading order QCD computation does confirm the presence of up to two powers of $\ln(M_H/m_c)$ in the interference contribution, their overall impact on the magnitude of QCD corrections to the interference turns out to be moderate due to a cancellation between double and single logarithmic terms.

KEYWORDS: Higgs Physics, Perturbative QCD, Quark Masses and SM Parameters

ARXIV EPRINT: 2102.04242

Contents

1 Introduction

Studies of Yukawa couplings play an important role in the verification of the mechanism of electroweak symmetry breaking as described by the Standard Model. By now, Higgs couplings to bottom and top quarks, as well as to tau leptons and muons, have been measured to a precision of about twenty percent [1–6]. Within the error bars, the measured values for all four Yukawa couplings are consistent with the Standard Model predictions.

However, the Yukawa couplings to lighter fermions have not been studied experimentally. Although it is generally agreed that the Yukawa couplings of electrons and up, down and strange quarks can be observed if and only if they deviate enormously from their Standard Model values, the situation with the charm Yukawa is not so hopeless. In fact, it appears that with the full LHC luminosity, the charm Yukawa coupling can be measured if its value deviates from the Standard Model expectation by an order one factor [7]. Different observables to measure the charm Yukawa coupling at the LHC have been proposed; they include inclusive ($H \to c\bar{c}$) and exclusive ($H \to J/\psi + \gamma$ and similar) decays of the Higgs boson [8–10], the modifications of the Higgs transverse momentum distribution [11] in the $gg \to H + X$ process and, finally, Higgs boson production cross section in association with a charm jet [12]. These indirect bounds on the charm Yukawa coupling were examined, for example, in ref. [13].

In this paper we focus on the latter process, $pp \to H + \mathrm{jet}_c$. At leading order in perturbative QCD, Higgs bosons are produced in association with charm jets in the partonic process $cg \to Hc$. The amplitude of this process receives contributions proportional to the charm Yukawa coupling and to an effective ggH coupling

$$\mathcal{M} \sim g_{\mathrm{Yuk}}\mathcal{M}_1 + g_{ggH}\mathcal{M}_2, \tag{1.1}$$

see figure 1. As a result, the $pp \to H + \mathrm{jet}_c$ cross section contains the interference term

$$\sigma_{Hc} \sim g_{\mathrm{Yuk}}^2\, \tilde{\sigma}_1 + g_{ggH}^2\, \tilde{\sigma}_2 + g_{\mathrm{Yuk}}g_{ggH}\, \tilde{\sigma}_{\mathrm{Int}}. \tag{1.2}$$

It can be expected that a reliable description of Higgs boson production in association with a charm jet can be obtained by systematically computing the different terms in eq. (1.2) to higher orders in perturbative QCD. In fact, it is emphasized in ref. [12] that the largest theoretical uncertainty in using $H+\mathrm{jet}_c$ production cross section to constrain charm Yukawa coupling is related to perturbative QCD uncertainties so that it seems natural to compute higher order QCD corrections to σ_{Hc} in eq. (1.2).

However, pursuing this program for the interference term in eq. (1.2) is quite subtle as we now discuss. Indeed, perturbative computations in QCD are performed with massless incoming partons. In case of the massless charm quark that, however, has non-vanishing Yukawa coupling to the Higgs boson, the interference term in eq. (1.2) vanishes and we obtain

$$\lim_{m_c \to 0} \sigma_{Hc} \sim g_{\mathrm{Yuk}}^2\tilde{\sigma}_1 + g_{ggH}^2\tilde{\sigma}_2. \tag{1.3}$$

This happens because the Yukawa interaction flips charm's helicity but the gluon-charm interaction conserves it; hence, the two contributions in eq. (1.1) cannot interfere if $m_c = 0$. For the massive charm quark the interference does not vanish and is proportional to the charm mass in the first power. Whether or not the interference contribution is negligible depends on the relative magnitude of the two amplitudes in eq. (1.1). Leading-order computations with massless quarks show that the charm-Yukawa independent amplitude $g_{ggH}\mathcal{M}_2$ in eq. (1.1) is larger than the charm-Yukawa dependent one $g_{\mathrm{Yuk}}\mathcal{M}_1$ suggesting that the interference may be non-negligible.

It is straightforward to calculate the interference at leading order in perturbative QCD. Indeed, the interference requires *one* helicity flip on a charm line that connects initial and final states; this flip is accomplished by a *single* mass insertion. This implies that one can compute the interference of the two amplitudes using massive charm quarks, take the $m_c \to 0$ limit and account for the first non-vanishing term proportional to m_c. Since we require a charm jet in the final state, none of the kinematic invariants of the $cg \to Hc$ process can be small. Hence, once one power of m_c is extracted, the rest of the leading-order calculation of the interference contribution can be performed using the standard approximation of massless (charm) quarks. Such calculation, that we describe in section 5, shows that the leading-order interference amounts to about ten percent of the contribution to the $H + \mathrm{jet}_c$ cross section that is proportional to the Yukawa coupling squared.

(a) Yukawa coupling.　　　　　　(b) Effective ggH vertex.
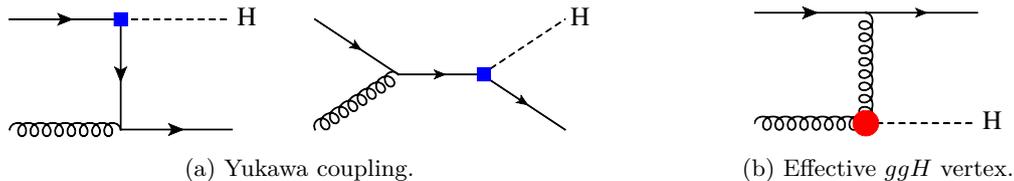
Figure 1. Leading-order Feynman diagrams contributing to the $pp \to Hc$ process. We distinguish two separate production mechanisms: one that is driven by the Yukawa coupling (left) and the other one that requires direct coupling of Higgs to gluons (right).

Although the interference contribution is not large, it is worth thinking about it at next-to-leading order (NLO) in perturbative QCD since there are reasons to believe that the interference contribution is *perturbatively unstable*, at variance with the two other contributions to $pp \to H + \mathrm{jet}_c$ cross section. Indeed, even if we require an energetic charm jet in the final state, soft and collinear kinematic configurations lead to logarithmic sensitivity of the interference to the charm mass m_c. Hence, before the $m_c \to 0$ approximation can be taken, the quasi-singular contributions proportional to logarithms of m_c have to be extracted from both real and virtual corrections to the interference part of the production cross section.[1]

One may argue that, since the finite charm mass provides yet another way to regulate collinear divergences, it is to be expected that the procedure described above will lead to a familiar picture of (quasi)-collinear factorization of QCD amplitudes. If so, all $\ln(m_c)$-dependent terms should disappear once infrared safe cross sections and distributions are computed using short-distance quantities, including conventional parton distribution functions (PDFs). However, we will show that for the interference contribution this expectation is invalid and that well-known formulas that describe *collinear* factorization of mass singularities are not applicable in that case. We will also show that the helicity flip leads to an appearance of *soft-quark* singularities that, interestingly, make jet algorithms logarithmically-sensitive to m_c.

There are two consequences of the above discussion. First, the problem of estimating the magnitude of the interference contribution to the production of a Higgs boson in association with a charm jet turns into an interesting problem in perturbative QCD that borders on such important issues as soft and collinear QCD factorization for mass power corrections [17–21]. Second, a more complex pattern of this factorization, as compared to the canonical collinear and soft cases [22], implies that NLO QCD corrections to leading-order interference are enhanced by up to two powers of a large logarithm $\ln Q/m_c$ where Q is a typical hard scale in the process $pp \to H + \mathrm{jet}_c$. It would be ideal to resum these logarithms but it is currently unknown how to do that. Therefore, the best we can do is to explicitly compute NLO QCD corrections to the interference. Although such an approach is limited

---

[1]We note that production of Higgs bosons in association with massive (bottom) quarks has been studied long time ago both in four- and five-flavor schemes [14–16]. Computations within the four-flavor scheme naturally include the interference of the Yukawa and ggH contributions but leave logarithms of the heavy quark mass unresummed. Calculations based on the five-flavor scheme naturally resum logarithms of the heavy quark mass but do not include the interference.

in scope, it allows us to expose logarithmically-enhanced contributions and estimate how significant they are for phenomenology.

Finally, since our approach involves dealing with massive quarks in the initial state, one may worry that its extension to next-to-next-to-leading (NNLO) and even higher perturbative orders is problematic because, starting from NNLO, QCD corrections to processes with massive partons in the initial state are known to be pathological, in that they are not infra-red finite [23–34]. Luckily, such worries are unfounded. Indeed, we note that the process studied in this paper is a result of a collision of a massive quark with a massless gluon and it is known that in this case the offending factorization violating terms, described e.g. in ref. [35], are absent.

Moreover, such factorization-violating effects, when present, are actually power-suppressed. In fact, they will first appear in NNLO terms that scale as $\alpha_s^2 m_c^4/s^2 \times d\sigma_{\mathrm{LO}}^{\mathrm{int}}$ where $d\sigma_{\mathrm{LO}}^{\mathrm{int}} \sim m_c^2/s^4$. However, our approach only works for terms that scale as $\alpha_s^n d\sigma_{\mathrm{LO}}^{\mathrm{int}}$, $n > 0$, modulo additional powers of $\ln m_c$. Therefore, even if such factorization-violation effects were present, extension of our approach to higher perturbative orders should be possible as long as we systematically omit power-suppressed terms.

The rest of the paper is organized as follows. In the next section we derive a relation between $\overline{\mathrm{MS}}$-regulated and mass-regulated parton distribution functions at $\mathcal{O}(\alpha_s)$ using the process of Higgs boson production in $c\bar{c}$ annihilation. We use the established relation to remove "conventional" collinear logarithms from NLO QCD corrections to the interference contribution to the production of Higgs boson in association with charm jet. In section 3 we discuss factorization of mass singularities in the interference contribution to $cg \to Hc$ process and show that it works differently as compared to the standard case [22]. In section 4 we briefly describe the technical details of the calculation of NLO QCD corrections to the interference contribution. In section 5 we present phenomenological results and discuss the relative importance of logarithmically-enhanced terms. We conclude in section 6. Additional discussion of soft and collinear limits of the interference contributions as well as some relevant soft integrals can be found in several appendices.

2 Matching parton distribution functions

Parton distribution functions are traditionally defined in the $\overline{\mathrm{MS}}$ scheme and employ massless on-shell partons. However, this is not the only option. In fact, the parton picture employs massless partons because hadronic hard scattering processes, properly defined, are insensitive to collinear and infra-red dynamics, up to power corrections. This implies that it should be possible to work with *any* collinear regulator in a consistent way.

A possible choice of a collinear regulator is a quark mass. This choice is very natural for our problem because, to study interference effects in the Higgs production, we have to start with a small but non-vanishing charm quark mass.

Parton distribution functions that employ quark masses as collinear regulators are not known phenomenologically. Hence, it becomes important for us to relate them to conventional $\overline{\mathrm{MS}}$ PDFs. We do this by requiring that "leading-twist" contributions to physical processes should be independent of collinear regulator. We can use this fact to derive

matching relations between parton distribution functions that are used for computations with nearly massive and strictly massless quarks.[2]

To derive a relation between "massive" and "massless" PDFs, we start with the production of a Higgs boson in an annihilation of two massive charm quarks and write the differential cross section as

$$d\sigma_{pp \to H} = \sum_{ij} \int dx_1 \, dx_2 \, f_i^{(m)}(x_1) f_j^{(m)}(x_2) d\hat\sigma_{ij \to H+X}^{(m)}. \tag{2.1}$$

Here $f_i^{(m)}$ are parton distribution functions and the superscript m implies that all relevant quantities should be computed using quark masses as collinear regulators. Also, $\hat\sigma_{ij \to H+X}^{(m)}$ is the partonic differential cross-section. At leading order $i(j) = c, \bar c$; at higher orders other channels also contribute.

Calculation at leading order in α_s is straightforward since the leading-order cross section $\sigma_{c\bar c \to H}^{(m)}$ has a regular $m_c \to 0$ limit. It follows that at leading order in α_s there is no difference between $f_i^{(m)}$ and conventional $\overline{\text{MS}}$ parton distribution functions, i.e. $f_i^{(m)} = f_i^{\overline{\text{MS}}}$.

The situation becomes more complicated at next-to-leading order where the charm quark mass screens collinear singularities; hence, our goal is to re-write the NLO QCD contributions to the cross section $c\bar c \to H + X$ in such a way that logarithms of m_c are extracted explicitly.

We begin by considering the process $c(p_1) + \bar c(p_2) \to H + g(p_3)$ and treating charm quarks as massive. Kinematic regions that lead to soft and (quasi-)collinear singularities are well understood. The behavior of matrix elements in these limits is described by conventional factorization formulas [22]. We can define a hard m_c-independent cross section by subtracting the singular limits. When the subtracted terms are added back and integrated over unresolved parts of the Hg phase space, logarithms of the charm mass appear. This procedure is identical to methods developed to extract infrared and collinear singularities from real emission contributions to partonic cross sections. Its application in the present context allows us to explicitly extract logarithms of the charm mass.

To organize the calculation, we follow the nested soft-collinear subtraction scheme [37–40] which, at next-to-leading order, is equivalent to the FKS scheme [41, 42]. We use dimensional regularization[3] to regularize soft singularities and the charm mass to regularize the collinear ones. Using notations from ref. [37], we write the partonic cross section for $c(p_1) + \bar c(p_2) \to H + g(p_3)$ as

$$
\begin{aligned}
2s \cdot d\hat\sigma_{c\bar c \to H+g} &= \int [dg_3] F_{\text{LM}}(1_c, 2_{\bar c}; 3_g) \equiv \langle F_{\text{LM}}(1_c, 2_{\bar c}; 3_g) \rangle = \langle S_3 F_{\text{LM}}(1_c, 2_{\bar c}; 3_g) \rangle \\
&+ \langle (C_{31} + C_{32})(I - S_3) F_{\text{LM}}(1_c, 2_{\bar c}; 3_g) \rangle + \langle (I - C_{31} - C_{32})(I - S_3) F_{\text{LM}}(1_c, 2_{\bar c}; 3_g) \rangle.
\end{aligned}
\tag{2.2}
$$

The key observation is that since the fully-regulated (last) term in eq. (2.2) is free of both soft and quasi-collinear singularities, the limit $m_c \to 0$ can be safely taken there. On

---

[2]We note that a derivation of the initial condition for the electron structure function in QED was recently presented in ref. [36]. There is a strong conceptual overlap of the discussion in that reference and the computation reported in this section. In particular, our procedure allows us to rederive elements that enter the structure functions in eqs. (4.121), (4.189) and (5.42) of ref. [36].

[3]The space-time dimension d is parametrized as $d = 4 - 2\epsilon$.

the contrary, both soft and collinear subtraction terms exhibit mass singularities; these mass singularities need to be extracted.

Consider the soft limit defined as $p_3 \cdot p_1 \sim p_3 \cdot p_2 \to 0$. It reads [22]

$$S_3 F_{\mathrm{LM}}(1_c, 2_{\bar{c}}; 3_g) \approx g_s^2 C_F \left(\frac{2(p_1 \cdot p_2)}{(p_1 \cdot p_3)(p_2 \cdot p_3)} - \frac{m_c^2}{(p_1 \cdot p_3)^2} - \frac{m_c^2}{(p_2 \cdot p_3)^2} \right) F_{\mathrm{LM}}(1_c, 2_{\bar{c}}), \quad (2.3)$$

where g_s is the unrenormalized strong coupling constant.

Since the soft gluon decouples from the function $F_{\mathrm{LM}}(1_c, 2_{\bar{c}})$ we can integrate eq. (2.3) over the gluon phase space. We work in the center-of-mass frame of the colliding charm partons and parametrize their energies as $E_1 = E_2 = E$. The center of mass energy squared in the massless approximation is then $s = 4E^2$. We also cut integrals over gluon energy at $E_3 = E_{\max}$, cf. ref. [37]. Integrating eq. (2.3) over gluon phase space $[\mathrm{d}g_3]$ and taking the $m_c \to 0$ limit, we find

$$\langle S_3 F_{\mathrm{LM}}(1_c, 2_c; 3_g) \rangle = -\frac{C_F [\alpha_s] E_{\max}^{-2\epsilon}}{\epsilon} [2\, I_{1m}(E) - I_{2m}(E)] \langle F_{\mathrm{LM}}(\tilde{1}_c, \tilde{2}_{\bar{c}}) \rangle, \quad (2.4)$$

where $[\alpha_s] = g_s^2 \Omega^{(d-2)} / (2(2\pi)^{d-1})$ and $\Omega^{(d-2)}$ is the solid angle of the $(d-2)$-dimensional space.[4] The notation $\tilde{1}_c(\tilde{2}_{\bar{c}})$ implies that the corresponding four-momenta should be taken in the massless approximation. The two integrals $I_{1m(2m)}$ in eq. (2.4) read

$$I_{1m}(E) = \int_{-1}^{1} \frac{\mathrm{d}\cos\theta (\sin^2\theta)^{-\epsilon}}{1 - \beta\cos\theta} \approx -\frac{4^{-\epsilon} \Gamma^2(1-\epsilon)}{\epsilon\, \Gamma(1-2\epsilon)} \left[1 - \frac{\Gamma(1+\epsilon)\Gamma(1-2\epsilon)}{\Gamma(1-\epsilon)} \left(\frac{m_c^2}{4E^2} \right)^{-\epsilon} \right],$$

$$I_{2m}(E) = \frac{m_c^2}{E^2} \int_{-1}^{1} \frac{\mathrm{d}\cos\theta (\sin^2\theta)^{-\epsilon}}{(1 - \beta\cos\theta)^2} \approx 2 \left(\frac{m_c^2}{E^2} \right)^{-\epsilon} \Gamma(1-\epsilon)\Gamma(1+\epsilon),$$

$$(2.5)$$

where $\beta = \sqrt{1 - m_c^2/E^2}$ and we neglected all power-suppressed terms when writing the results.

Collinear subtraction terms contain quasi-collinear singularities. The two collinear limits correspond to two distinct cases, $p_1 \cdot p_3 \sim m_c^2 \to 0$ and $p_2 \cdot p_3 \sim m_c^2 \to 0$. They read

$$C_{3i}\, F_{\mathrm{LM}}(1_c, 2_{\bar{c}}; 3_g) = \frac{g_s^2}{(p_i \cdot p_3)} \left[P_{qq}(z) - \frac{C_F m_c^2 z}{(p_i \cdot p_3)} \right] \frac{F_{\mathrm{LM}}^{(i)}(\tilde{1}_c, \tilde{2}_{\bar{c}}; z)}{z}, \quad (2.6)$$

where

$$F_{\mathrm{LM}}^{(i)}(\tilde{1}_c, \tilde{2}_{\bar{c}}; z) = \delta_{i1}\, F_{\mathrm{LM}}(z \cdot \tilde{1}_c, \tilde{2}_{\bar{c}}) + \delta_{i2}\, F_{\mathrm{LM}}(\tilde{1}_c, z \cdot \tilde{2}_{\bar{c}}), \quad (2.7)$$

and

$$P_{qq}(z) = C_F \left(\frac{1+z^2}{1-z} - \epsilon(1-z) \right) \quad (2.8)$$

---

[4]The solid angle of the d-dimensional space is $\Omega^{(d)} = 2\pi^{d/2}/\Gamma(d/2)$.

is the collinear splitting function. The variable z is defined as $z = (E_i - E_3)/E_i$ with $i = 1, 2$, as appropriate.

Since, when computing the collinear limits, we do not change the gluon phase space [37], integrated collinear subtraction terms are still described by angular integrals $I_{1m(2m)}$ shown in eq. (2.5). Performing the soft subtraction of the collinear-subtracted cross section, we find

$$\langle C_{31}(I - S_3) F_{\mathrm{LM}}(1_c, 2_{\bar{c}}; 3_g) \rangle = [\alpha_s] E^{-2\epsilon} \int_0^1 dz\, \mathcal{I}(E, z)\, \left\langle \frac{F_{\mathrm{LM}}(z \cdot \tilde{1}_c, \tilde{2}_{\bar{c}})}{z} \right\rangle, \qquad (2.9)$$

where

$$\mathcal{I}(E, z) = I_{1m}(E)\, \bar{P}_{qq}(z) - I_{2m}(E)\, \bar{P}_{qq}^{(m)}(z), \qquad (2.10)$$

and

$$\bar{P}_{qq} = C_F \left(\frac{1 + z^2}{(1 - z)^{1 + 2\epsilon}} - \epsilon(1 - z)^{1 - 2\epsilon} + \frac{1}{\epsilon} \delta(1 - z) e^{-2\epsilon L_1} \right),$$
$$\bar{P}_{qq}^{(m)} = C_F \left(\frac{z}{(1 - z)^{1 + 2\epsilon}} + \frac{1}{2\epsilon} \delta(1 - z) e^{-2\epsilon L_1} \right), \qquad (2.11)$$

and $L_1 = \ln(E_{\max}/E)$. A similar expression can be written for $\langle C_{32}(I - S_3) F_{\mathrm{LM}}(1, 2; 3) \rangle$.

It is straightforward to combine soft and collinear contributions and to expand them in ϵ. At this point, it is convenient to switch to a strong coupling constant renormalized at the scale μ. We obtain

$$\langle S_3 F_{\mathrm{LM}}(1, 2; 3) \rangle + \langle C_{31}(I - S_3) F_{\mathrm{LM}}(1, 2; 3) \rangle + \langle C_{32}(I - S_3) F_{\mathrm{LM}}(1, 2; 3) \rangle =$$
$$= C_F \frac{\alpha_s(\mu)}{2\pi} \left\{ -\frac{2 L_c}{\epsilon} - L_c^2 + 1 - \frac{2\pi^2}{3} - 3 L_c + 2 L_c \ln \frac{M_H^2}{\mu^2} \right\} \langle F_{\mathrm{LM}}(1, 2) \rangle$$
$$+ C_F \frac{\alpha_s(\mu)}{2\pi} \int_0^1 dz \left\{ \left[\frac{1 + z^2}{1 - z} \right]_+ L_c + (1 - z) \right\} \left\langle \frac{F_{\mathrm{LM}}(z \cdot \tilde{1}_c, \tilde{2}_{\bar{c}})}{z} + \frac{F_{\mathrm{LM}}(\tilde{1}_c, z \cdot \tilde{2}_{\bar{c}})}{z} \right\rangle, \qquad (2.12)$$

where $L_c = \ln(M_H^2/m_c^2) - 1$.

To determine full NLO QCD correction to $c\bar{c} \to H$ cross section, we need to include virtual corrections. They are computed in a standard way (see e.g. ref. [43] where such a computation is reported); the result is then expanded around $m_c = 0$. We renormalize the Yukawa coupling in the $\overline{\mathrm{MS}}$ scheme at the scale μ. The result reads

$$2s \cdot d\hat{\sigma}_V = C_F \frac{\alpha_s(\mu)}{2\pi} \left[\frac{2}{\epsilon} L_c + \frac{4\pi^2}{3} + 4 + L_c^2 + (2 L_c + 3) \ln \frac{\mu^2}{M_H^2} + 3 L_c \right] \langle F_{\mathrm{LM}}(\tilde{1}_c, \tilde{2}_{\bar{c}}) \rangle. \qquad (2.13)$$

Upon combining virtual, soft, collinear and fully-regulated terms, we obtain the following NLO QCD contribution to $c\bar{c} \to H + X$ cross section

$$2s \cdot d\hat{\sigma}_{\rm NLO} = \langle (I - C_{31} - C_{32})(I - S_3) F_{\rm LM}(\tilde{1}_c, \tilde{2}_{\bar{c}}; 3_g) \rangle$$
$$+ C_F \frac{\alpha_s(\mu)}{2\pi} \left(\frac{2\pi^2}{3} + 5 - 3\ln \frac{M_H^2}{\mu^2} \right) \langle F_{\rm LM}(\tilde{1}_c, \tilde{2}_{\bar{c}}) \rangle \tag{2.14}$$
$$+ \frac{\alpha_s(\mu)}{2\pi} \sum_{i=1}^{2} \int_0^1 dz \left\{ P_{qq}^{AP}(z) \ln \frac{\mu^2}{m_c^2} + P_{qq}^{\rm fin}(z) \right\} \left\langle \frac{F_{\rm LM}^{(i)}(\tilde{1}_c, \tilde{2}_{\bar{c}}; z)}{z} \right\rangle,$$

where

$$P_{qq}^{\rm AP} = C_F \left[\frac{1+z^2}{1-z} \right]_+ \quad \text{and} \quad P_{qq}^{\rm fin} = C_F \left[\frac{1+z^2}{1-z} \right]_+ \left(\ln \frac{M_H^2}{\mu^2} - 1 \right) + C_F(1-z). \tag{2.15}$$

The first term on the right hand side of eq. (2.14) is the hard inelastic contribution; it can be computed directly in the massless limit, $m_c = 0$. The second term on the right hand side of eq. (2.14) is the soft-virtual piece; it describes kinematic configuration that is equivalent to the leading-order one. The third term in eq. (2.14) describes kinematic configurations that are boosted relative to the leading-order ones; we note that the residual logarithmic dependence on m_c is present in these contributions *only*.

A similar computation for *massless* charm partons requires, in addition, a collinear PDF renormalization to make the partonic cross section collinear-finite and independent of the regularization parameter ϵ. The result reads

$$2s \cdot d\hat{\sigma}_{\rm NLO}^{m_c=0} = \langle (I - C_{31} - C_{32})(I - S_3) F_{\rm LM}(\tilde{1}_c, \tilde{2}_{\bar{c}}; 3_g) \rangle$$
$$+ C_F \frac{\alpha_s(\mu)}{2\pi} \left[5 + \frac{2\pi^2}{3} - 3\ln \frac{M_H^2}{\mu^2} \right] \langle F_{\rm LM}(\tilde{1}_c, \tilde{2}_{\bar{c}}) \rangle \tag{2.16}$$
$$+ \frac{\alpha_s(\mu)}{2\pi} \sum_{i=1}^{2} \int_0^1 dz \, P_{qq}^{(\epsilon)}(z) \left\langle \frac{F_{\rm LM}^{(i)}(\tilde{1}_c, \tilde{2}_{\bar{c}}; z)}{z} \right\rangle,$$

where

$$P_{qq}^{(\epsilon)}(z) = C_F \left[\frac{1+z^2}{1-z} \right]_+ \ln \frac{M_H^2}{\mu^2} + 2C_F \left[\frac{1+z^2}{1-z} \ln(1-z) \right]_+ + C_F(1-z). \tag{2.17}$$

The partonic cross sections in eqs. (2.14) and (2.16) should be convoluted with *different* parton distribution functions to obtain hadronic cross sections: in case of eq. (2.16) we must use conventional $\overline{\rm MS}$ PDFs whereas in case when the incoming charm quarks are massive a special set of PDFs is required. Nevertheless, since m_c is just a collinear regulator, results for short-distance hadronic cross sections should be the same, independent of whether one starts with nearly massive or massless charm quarks. This requirement allows us to derive a relation between the "massive" and the $\overline{\rm MS}$ PDFs. It reads

$$f_a^{(m)} = \hat{O}_{ab} \otimes f_b^{\overline{\rm MS}}, \tag{2.18}$$

where

$$\hat{O}_{ab}(z) = \delta_{ab}\delta(1-z) + \left(\frac{\alpha_s}{2\pi}\right) G_{ab}(z) + \dots . \tag{2.19}$$

The computation that we just described allows us to determine the coefficient $G_{cc}(z)$. We find

$$G_{cc}(z) = -\ln\left(\frac{\mu^2}{m_c^2}\right) P_{qq}^{\mathrm{AP}}(z) + C_F \left[\frac{1+z^2}{1-z}(1 + 2\ln(1-z))\right]_+ . \tag{2.20}$$

We can also compute "off-diagonal" coefficients G_{ab} that involve charm quark and gluon PDFs; they are important for removing mass singularities that arise in $g \to c$ and $c \to g$ transitions. Computations proceed along the same lines as described above except that we employ other partonic processes for the analysis. Namely, we derive a relation for $g \to c$ transition by considering a $cg \to Hc$ process in a theory where only Yukawa coupling is present and no direct ggH coupling is allowed. To derive a relation for $c \to g$ transition, we again consider $cg \to Hc$ process but now only allow for the ggH coupling. In both cases only (quasi)-collinear singularities are present; this simplifies the required computations significantly. We find

$$G_{cg}(z) = -\ln\left(\frac{\mu^2}{m_c^2}\right) P_{qg}^{\mathrm{AP}}(z),$$
$$G_{gc}(z) = -\left[\ln\left(\frac{\mu^2}{m_c^2}\right) - 2\ln(z) - 1\right] P_{gq}^{\mathrm{AP}}(z), \tag{2.21}$$

where

$$P_{qg}^{\mathrm{AP}} = T_R\left[1 - 2z(1-z)\right], \quad P_{gq}^{\mathrm{AP}} = C_F \frac{1 + (1-z)^2}{z}. \tag{2.22}$$

The results for the functions $G_{ab}(z)$ reported in eqs. (2.20), (2.21) are important for the calculation of NLO QCD corrections to the interference contribution to Higgs boson production in association with a charm jet. Indeed, as explained in the Introduction, to access the interference, we need to start with the massive incoming charm quarks and carefully study the massless limit. Since the charm mass serves as a collinear regulator, we are forced to use parton distribution functions $f_i^{(m)}$. We then use the relation eq. (2.18) to express these functions through the conventional $\overline{\mathrm{MS}}$ PDFs and, in doing so, remove logarithms of m_c that are associated with the radiation by the incoming charm quarks. Because the interference contribution to $pp \to H + \mathrm{jet}_c$ involves a helicity flip, standard collinear logarithms associated with initial state emissions are not the only logarithms of the charm mass that appear in the cross section. We elaborate on this statement in the next section.

3 Interference contributions and factorization in the quasi-collinear limit

The discussion in the previous section shows that the dependence on m_c disappears from hard cross sections provided that conventional factorization formulas for soft and quasi-collinear singularities, eqs. (2.3), (2.6), hold true. However, since the interference contribution requires a helicity flip, its soft and quasi-collinear limits are different from the

conventional ones. As we explain below, such limits can still be described by simpler matrix elements but these matrix elements do not always correspond to processes with reduced multiplicities of final state particles.

To discuss and illustrate these subtleties in more detail, consider the process

$$c(p_1) + g(p_2) \longrightarrow H(p_H) + c(p_3) + g(p_4). \tag{3.1}$$

The first point that needs to be emphasized is that, if we work with a finite charm mass, *true* soft and collinear limits of the process in eq. (3.1) are, in fact, conventional. These contributions can be extracted and combined with the virtual corrections to $cg \to Hc$ and renormalized gluon parton distribution function giving a finite result for the partonic cross section. Such a procedure is identical to what is usually done in NLO QCD computations [41, 42, 44] that are traditionally performed using dimensional regularization for soft and collinear divergences. However, cancellation of "true" infrared and collinear divergences does not tell us anything about non-analytic dependence of partonic cross sections on the charm mass that we need to extract before taking the $m_c \to 0$ limit.

In this paper, we adopt a pragmatic approach and extract all the terms that are singular in the $m_c \to 0$ limit by studying interference contributions to squares of scattering amplitudes, computed *explicitly* with massive charm quarks, for all relevant partonic processes, $cg \to Hcg$, $gg \to Hc\bar{c}$, $cq \to Hcq$, $cc \to Hcc$, $c\bar{c} \to Hc\bar{c}$. In that sense, we do not attempt to develop an understanding of infrared and quasi-collinear factorization for generic processes that involve a helicity flip. However, to illustrate main differences with the conventional collinear factorization we discuss an emission of a collinear gluon off an incoming charm quark in case of the interference contribution in some detail.

To this end, we consider the process in eq. (3.1) in the quasi-collinear limit $p_1 \cdot p_4 \sim m_c^2$. To describe this limit, we divide the amplitude for the full process $cg \to Hcg$ into two parts

$$\mathcal{M} = \mathcal{M}_{\text{sing}} + \mathcal{M}_{\text{fin}}, \tag{3.2}$$

where $\mathcal{M}_{\text{sing}}$ refers to diagrams where the gluon is emitted off the incoming quark with the momentum p_1 and $\mathcal{M}_{\text{fin}}$ refers to the remaining diagrams. The first contribution ($\mathcal{M}_{\text{sing}}$) is singular in the $p_1 \cdot p_4 \sim m_c^2 \to 0$ limit whereas the second one ($\mathcal{M}_{\text{fin}}$) is not.

Upon squaring the amplitude, eq. (3.2), and summing over polarizations of initial and final state particles, we obtain

$$\sum_{\text{pol}} |\mathcal{M}|^2 = \sum_{\text{pol}} |\mathcal{M}_{\text{sing}}|^2 + \sum_{\text{pol}} \left(\mathcal{M}_{\text{sing}} \mathcal{M}_{\text{fin}}^\dagger + \text{h.c.} \right) + \dots, \tag{3.3}$$

where the ellipsis stands for contributions that are finite in the $p_1 \cdot p_4 \sim m_c^2 \to 0$ limit. We note that the product of singular and non-singular contributions to the amplitude squared that we retain in eq. (3.3) is known to be non-singular in the conventional quasi-collinear limits provided that physical polarizations are used to describe the emitted gluon. As we will show below, this is *not the case* for the interference contributions considered in this paper.

To extract the quasi-collinear singularities from the square of the amplitude in eq. (3.3) we need to analyze the quasi-collinear kinematics; for this analysis there is no difference

between helicity-conserving and helicity-flipping contributions. Indeed, following the standard approach, we re-write the four-momentum of the incoming charm quark and the four-momentum of the emitted gluon through massless momenta $\tilde{p}_1$ and p_2 and find

$$p_1 = \left(1 - \frac{m_c^2}{s}\right)\tilde{p}_1 + \left(\frac{m_c^2}{s}\right)p_2 + \mathcal{O}(m_c^4)\,, \qquad p_4 = (1-z)\tilde{p}_1 + yp_2 + p_{4,\perp}\,. \tag{3.4}$$

In the above equation, $s = 2\tilde{p}_1 \cdot p_2$ and $p_{4,\perp} \cdot \tilde{p}_1 = p_{4,\perp} \cdot p_2 = 0$. We use the on-shell condition $p_4^2 = 0$ and obtain

$$y = -\frac{p_{4,\perp}^2}{(1-z)s}\,. \tag{3.5}$$

It follows that

$$2p_1 \cdot p_4 \approx s\left((1-z)\frac{m_c^2}{s} + y\right) = \frac{1}{1-z}\left((1-z)^2 m_c^2 - p_{4,\perp}^2\right)\,. \tag{3.6}$$

We conclude that the kinematic region where $p_{4,\perp}^2 \sim m_c^2$ provides unsuppressed contributions to the cross section in the $m_c \to 0$ limit.

We write the singular contribution as follows

$$\mathcal{M}_{\text{sing}} = -g_s t_{i_c i_1}^{a_4} \hat{\mathcal{A}}_{\text{sing}}^{i_c} \frac{\hat{p}_1 - \hat{p}_4 + m_c}{2(p_1 \cdot p_4)} \,\hat{\epsilon}_4 \,u(p_1)\,, \tag{3.7}$$

and use the decomposition of the four-momenta $p_{1,4}$ given in eq. (3.4) to obtain

$$\mathcal{M}_{\text{sing}} = \frac{g_s t_{i_c i_1}^{a_4}}{2(p_1 \cdot p_4)}\hat{\mathcal{A}}_{\text{sing}}^{i_c}\left[-\frac{2p_{4,\perp} \cdot \epsilon_4}{1-z} + \hat{\epsilon}_4\left(m_c(1-z) + \hat{p}_{4,\perp} + \kappa\hat{p}_2\right)\right]u(p_1)\,. \tag{3.8}$$

In eq. (3.8), we introduced a parameter κ defined as

$$\kappa = -\frac{m_c^2(1-z)}{s} - \frac{p_{4,\perp}^2}{s(1-z)}\,. \tag{3.9}$$

We note that in deriving eq. (3.8) we have used $p_4 \cdot \epsilon_4 = 0$ and the gauge fixing condition $p_2 \cdot \epsilon_4 = 0$.

The result for the singular contribution, eq. (3.8), is generic; it does not distinguish between helicity-conserving and helicity-flipping contributions. However, it is easy to see that there is a difference between the two. For example, since the helicity-flipping contribution requires one *additional* power of m_c, one can convince oneself that a combination of terms labeled as κ in eq. (3.9) may contribute to the collinear limit of the interference but it cannot contribute to the collinear limit of the helicity-conserving amplitudes.

Hence, performing standard manipulations and paying attention to subtleties indicated above, we obtain the contribution to the interference that is non-analytic in the $m_c \to 0$

limit. It reads

$$
\lim_{p_1 \cdot p_4 \to 0} \mathrm{Int}\left[\mathcal{M}^2(1_c, 2_g; 3_c, 4_g)\right] = g_s^2 \Bigg[\left(\frac{P_{qq}(z)}{(p_1 \cdot p_4)} - \frac{C_F m_c^2 z}{(p_1 \cdot p_4)^2}\right) \mathrm{Int}\left[\frac{|\mathcal{M}(z1_c, 2_g; 3_c)|^2}{z}\right]
$$

$$
- \frac{C_F m_c (1-z)}{z(p_1 \cdot p_4)} \mathrm{Int}\left[\mathrm{Tr}\left[\hat{\mathcal{A}}^{i_c}(z \cdot \tilde{1}_c, 2_g; \tilde{3}_c)\hat{\mathcal{A}}^{i_c,\dagger}(z \cdot \tilde{1}_c, 2_g; \tilde{3}_c)\right]\right]\Bigg]
$$

$$
+ g_s C_F \frac{(1-z)m_c}{2(p_1 \cdot p_4)}\mathrm{Int}\left[\mathrm{Tr}\left[\hat{p}_1 \mathcal{A}^{i_c}(z \cdot \tilde{1}_c, 2_g; \tilde{3}_c)\hat{\mathcal{A}}_{\mathrm{fin}}^{i_c,\dagger}(\tilde{1}_c, 2_g; \tilde{3}_c, (1-z)\cdot\tilde{1}_g)\hat{\epsilon}_4 + \mathrm{h.c.}\right]\right]. \tag{3.10}
$$

It is understood that $\mathrm{Int}[\ldots]$ extracts the interference contributions from the relevant quantities; sums over colors and polarizations are implicit. The quantities $\mathcal{A}$ are related to amplitudes $\mathcal{M}$ in the following way

$$
\mathcal{M}(\tilde{1}_c, 2_g; \tilde{3}_c) = \hat{\mathcal{A}}^{i_1}(\tilde{1}_c, 2_g; \tilde{3}_c)\, u(\tilde{p}_1), \quad \mathcal{M}_{\mathrm{fin}}(\tilde{1}_c, 2_g; \tilde{3}_c, 4_g) = \hat{\mathcal{A}}_{\mathrm{fin}}^{i_1}(\tilde{1}_c, 2_g; \tilde{3}_c, 4_g)\, u(\tilde{p}_1). \tag{3.11}
$$

They have to be computed in the $m_c = 0$ limit.[5]

It is instructive to discuss the origin of the different terms in eq. (3.10). The first term on the right-hand side of eq. (3.10) contains the leading-order interference multiplied with the standard massive collinear splitting function; this is the conventional quasi-collinear limit applied to the interference. If only this term were present in eq. (3.10), there would be no differences in the collinear factorization between helicity-changing and helicity-conserving contributions.

The second and the third terms on the right-hand side of eq. (3.10) are new structures; they appear because the required helicity flip can occur on the *external charm quark lines*. To illustrate this point, we square the first equation in eq. (3.11), sum over polarizations and find

$$
\sum_{\mathrm{spins}} |\mathcal{M}(1_c, 2_g; 3_c)|^2 = \mathrm{Tr}\left[(\hat{p}_1 + m_c)\hat{\mathcal{A}}^{i_c}\hat{\mathcal{A}}^{i_c,\dagger}\right]. \tag{3.12}
$$

The interference requires a helicity flip that is facilitated by a single mass insertion. The above equation shows that this mass insertion can occur either in the $(\hat{p}_1 + m_c)$ density matrix of the external quark or "inside" the $\hat{\mathcal{A}}\hat{\mathcal{A}}^\dagger$ term. The structure that appears in the second term on the right hand side of eq. (3.10) originates from the mass term in the density matrix. Once the mass term is extracted, the rest can be computed in the massless approximation. We find

$$
\mathrm{Int}\left[\mathrm{Tr}\left[(\hat{p}_3 + m_c)\hat{\mathcal{A}}^{i_c}(1_c, 2_g; 3_c)\hat{\mathcal{A}}^{i_c,\dagger}(1_c, 2_g; 3_c)\right]\right] \to
$$
$$
m_c \,\mathrm{Int}\left[\mathrm{Tr}\left[\hat{\mathcal{A}}^{i_c}(\tilde{1}_c, 2_g; \tilde{3}_c)\hat{\mathcal{A}}^{i_c,\dagger}(\tilde{1}_c, 2_g; \tilde{3}_c)\right]\right]. \tag{3.13}
$$

_____

[5]We remind the reader that the notation $\tilde{i}$ implies that a light-cone four-momentum of a particle i must be used in the computation.

The last term on the right hand side in eq. (3.10) describes a quasi-collinear singularity that originates from the interference of singular and regular contributions in eq. (3.3); it is particular to the helicity-flipping case and does not appear in the conventional collinear limits. As a consequence, this contribution still depends on the part of the reduced matrix element of the original $2 \to 3$ process calculated in the strict collinear limit of the incoming massless charm quark and the emitted gluon.

We emphasize once again that eq. (3.10) shows clear differences between conventional factorization of quasi-collinear singularities and the factorization in case of the helicity flip. These differences lead to a peculiar structure of the logarithms of the charm quark mass in the interference contribution as they do not follow canonical pattern and cannot be removed by a transition to $\overline{\text{MS}}$ parton distribution functions. In addition, we also find that the interference contributions exhibit *quasi-soft* quark singularities that also lead to logarithms of the charm mass. Although it would be interesting to understand factorization of mass singularities in processes with the helicity flip from a more general perspective, our strategy for now is to *explicitly* compute all relevant contributions within fixed-order perturbation theory extracting all non-analytic m_c-dependent terms along the way. Additional details of our approach can be found in several appendices.

4 Technical details of the calculation

In this section we briefly describe calculation of one-loop and real emission contributions to the interference part of the $cg \to Hc$ process. We begin with the discussion of the virtual corrections.

We compute the relevant one-loop diagrams keeping charm-quark masses finite. We employ the standard Passarino-Veltman reduction [45] to express the $cg \to Hc$ amplitude in terms of one-loop scalar integrals.[6] After computing the one-loop contribution to the interference, we expand the expression around $m_c = 0$ and keep the leading $\mathcal{O}(m_c)$ term in this expansion.[7] The one-loop amplitudes contain ultraviolet and infrared singularities. The ultraviolet singularities are removed by the renormalization. We closely follow the discussion in appendix A of ref. [43] where many of the required renormalization constants are presented. Similar to ref. [43], we renormalize the charm-quark mass in the on-shell scheme but employ the $\overline{\text{MS}}$ renormalization for the Yukawa coupling constant. In addition to the discussion in that reference, we require the one-loop renormalization constant of the effective ggH vertex that we take from ref. [46]. After the ultraviolet renormalization is performed, the $cg \to Hc$ amplitude still contains $1/\epsilon$ poles of infrared origin. These poles satisfy the Catani's formula [47] and cancel with similar poles in real emission contributions to the partonic cross section.

According to the discussion in section 3, factorization of quasi-collinear and quasi-soft singularities in the interference contribution is not canonical. This implies that even if we take the $m_c \to 0$ limit and switch to $\overline{\text{MS}}$ parton distribution functions, the NLO QCD

---

[6]We use `FeynCalc` [48, 49] for a cross-check of our computation.

[7]We employed the Package-X program [50] for numerical checks of scalar integrals and their $m_c \to 0$ expansion.

corrections to the interference still contain logarithms of the charm mass. Since it is currently unknown how these logarithms can be resummed, we follow a pragmatic approach. Namely, we compute relevant virtual and real emission contributions, extract from them logarithms of the charm mass and take the $m_c \to 0$ limit once the mass logarithms have been extracted. To accomplish this, we construct subtraction terms for the real emission contributions for soft, collinear, quasi-collinear and quasi-soft singularities by direct inspection of the relevant matrix elements. The subtraction terms are then integrated over unresolved real emission phase space and combined with the PDF renormalization, including the transition from "massive" to $\overline{\text{MS}}$ PDFs, and the virtual corrections.

We emphasize that the transformation from "massive" to conventional $\overline{\text{MS}}$ parton distribution functions is important in our construction because "massive" PDFs are not known phenomenologically and, as we have shown in section 2, the two PDFs start being different at order $\mathcal{O}(\alpha_s)$. Moreover, we stress that in addition to allowing us to use well-defined inputs in our computation, this transformation incidentally resums some logarithms of the charm quark mass. Unfortunately, this transformation does not resum *all* logarithms of the charm quark mass because of more complicated factorization pattern. This is definitely a limitation for our approach but it is the best we can do at the moment.

The only difference with respect to the canonical procedure for NLO QCD computations is that in our case the subtraction terms are directly obtained from the squared amplitude and are not written in terms of easily recognizable universal functions; see section 3 and appendix A for further details. In particular, even contributions that are enhanced by *two* powers of a logarithm of the charm mass, $\mathcal{O}(\alpha_s \ln^2(m_c))$, do not appear to be proportional to the leading-order interference contribution to the cross section. As we observed when studying the collinear limit for the interference term in section 3, the collinear factorization formula changes implying that it is possible to flip helicity on external lines which leads to new structures that are not captured by conventional collinear factorization. Since it is not known how to resum such contributions and how to associate them with structures related to initial partons, the best we can do here is to extract $\ln(m_c)$-dependencies for these contributions. Although this approach is limited in scope, it allows us to expose such logarithmic terms and estimate how significant they are for phenomenology.

5 Numerical results

To present numerical results we consider proton-proton collisions at 13 TeV. We take $M_H = 125\,\text{GeV}$ for the Higgs-boson mass and $m_c = 1.3\,\text{GeV}$ for the pole mass of the charm quark. The charm Yukawa coupling is calculated using the $\overline{\text{MS}}$ charm mass, $\overline{m}_c(M_H) = 0.81\,\text{GeV}$.[8] We use `NNPDF31_lo_as_0118` and `NNPDF31_nlo_as_0118` parton distribution functions [51, 52] for leading and next-to-leading order computations, respectively. The value of the strong coupling constant α_s is calculated using dedicated routines provided with NNPDF sets.

---

[8]We use program `RunDec` [53, 54] to compute the value of the running charm quark mass.

(a) Fiducial cross section (LO).

(b) Interference/Yukawa ratio.
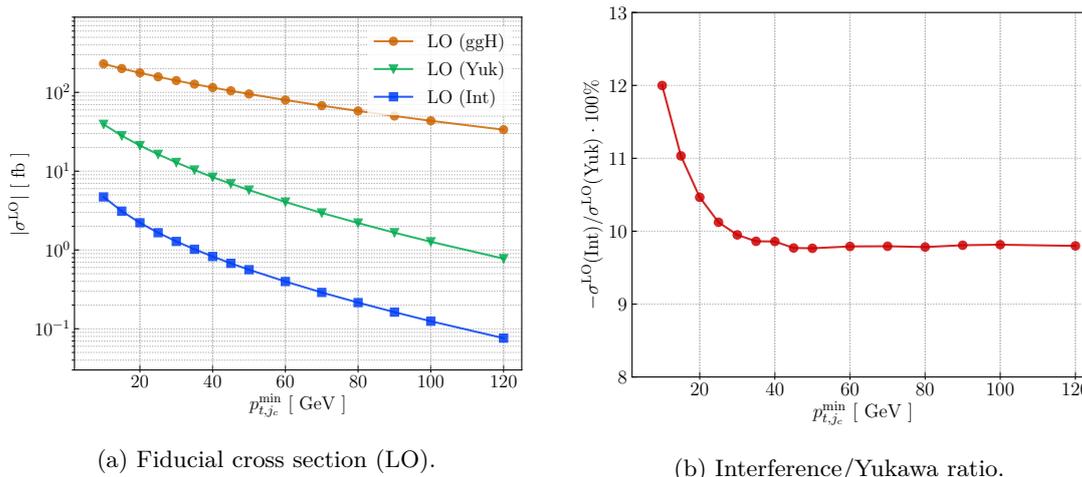
Figure 2. Leading-order cross sections computed for different values of the charm-jet p_t-cut. We show Yukawa-like (green) and ggH-like (orange) contributions as well as the *absolute value* of the interference (blue). In the right pane the ratio of the interference and the Yukawa-like fiducial cross section are shown.

To define jets we use standard anti-$k_\perp$ algorithm with $\Delta R = 0.4$; charm jets are required to contain at least one c or $\bar{c}$ quark. For numerical computations we require at least one charm jet with $p_{t,j} > 20\,\text{GeV}$ and $|\eta_j| < 2.5$. Moreover, we demand that the charm parton inside the charm jet carries at least 75% of the jet's transverse momentum.[9] The latter requirement removes kinematic cases where a soft charm is clustered together with a hard gluon into a charm jet in spite of a large angular separation between the two. Since, as we explained earlier, our calculation is logarithmically sensitive to *soft emissions of charm quarks*, defining charm jets with an additional cut on the charm quark transverse momentum allows us to avoid jet-algorithm dependent logarithms of m_c that may appear otherwise. We note that we apply all these requirements even in the subtraction terms where c and $\bar{c}$ momenta are computed in the collinear and/or soft approximations.

We start by presenting fiducial cross sections for the three terms in eq. (1.2) separately. Central values for all the cross sections presented below correspond to the renormalization and factorization scales set to $\mu_F = \mu_R = \mu = M_H$; subscripts and superscripts indicate shifts in central values if $\mu = M_H/2$ and $\mu = 2M_H$ are used in the calculation. At leading order, we find

$$\sigma_{ggH}^{\text{LO}} = 176.6^{+47.6}_{-36.5}\,\text{fb}\,, \qquad \sigma_{\text{Yuk}}^{\text{LO}} = 21.22^{+1.47}_{-1.67}\,\text{fb}\,, \qquad \sigma_{\text{Int}}^{\text{LO}} = -2.21^{+0.29}_{-0.31}\,\text{fb}\,, \qquad (5.1)$$

for the ggH-dependent cross section, the Yukawa-dependent cross section and the interference, respectively. In figure 2 we show the comparison between $\mu = M_H$ cross sections and the interference in dependence on the cut of the charm jet transverse momentum. We observe that the ratio of the interference to the Yukawa-dependent contribution is about ten percent for all values of the $p_{t,j}$-cut.

---

[9] If more than one c or $\bar{c}$ parton is clustered into a jet, we apply this requirement to the hardest of them.

$\Delta\sigma^{\mathrm{NLO}}$ [fb]	cg	cq	gg	cc	$c\bar{c}$	PDF	sum
const.	-1.63	0.13	2.33	0.01	-0.01	0.11	0.94
L	2.23	—	-6.33	-0.04	0.01	1.66	-2.47
L^2	-0.06	—	2.66	0.01	-0.08	—	2.52
total	0.54	0.13	-1.34	-0.02	-0.08	1.76	1.00

Table 1. The NLO QCD corrections to the interference split according to partonic channels. The results are given in femtobarns. The column marked "PDF" refers to the PDF-scheme change discussed in section 2. For each partonic channel we show $\mathcal{O}(L^2)$, $\mathcal{O}(L)$ and $\mathcal{O}(L^0)$ contributions where $L = \ln(M_H/m_c)$.

At next-to-leading order the fiducial cross section for the interference term becomes

$$\sigma^{\mathrm{NLO}}_{\mathrm{Int}} = -1.024(5)^{+0.224}_{-0.144} \text{ fb} \,. \tag{5.2}$$

It follows from eqs. (5.1), (5.2) that the NLO QCD corrections decrease the absolute value of the leading-order interference by about fifty percent. The scale uncertainty appears to be reduced by about a factor 2. The NLO result for the interference is outside the leading-order scale-uncertainty interval, cf. eqs. (5.1), (5.2), emphasizing the fact that the appearance of the logarithms of the charm mass in NLO QCD corrections to the interference makes the scale variation uncertainty of the leading-order result a very poor indicator of the theoretical uncertainty in this case.

It is instructive to separate the NLO contributions to the interference into parts that are independent of m_c and parts that are logarithmically enhanced for all the partonic channels. The relevant results are shown in table 1. We find that the largest contribution at NLO comes from the gluon-gluon channel which is enhanced by the large gluon luminosity. Also, the charm-gluon (cg) and the charm-quark channels (cq) provide relatively large contributions.[10] Note that the (cq) channel is free of logarithmic contributions since there are no singular limits that involve charm quarks. Contributions related to the PDF transformation do not feature the double-logarithmic part since the $\mathcal{O}(\ln^2 m_c)$ terms originate exclusively from soft-collinear limits that involve c-quarks.

It follows from table 1 that double-logarithmic terms and single-logarithmic terms provide nearly equal, but opposite in sign, contributions to the NLO QCD interference. This cancellation between terms with different parametric dependence on m_c should be considered as an artifact but it does emphasize that studying *only* the leading logarithmic $\mathcal{O}(\ln^2 m_c)$ contribution in this case is insufficient for phenomenology. We also note that the $\mathcal{O}(\ln^2 m_c)$ term in the cg channel is quite small reflecting the fact that there is a very strong — but incomplete — cancellation between double-logarithmic contributions to

---

[10]Here, by "quark" we mean any quark of a flavor other than c. There is a subtlety related to the b-quark contribution because b-quarks have stronger interactions with Higgs bosons as compared to charm quarks. Such contributions can, presumably, be dealt with using b anti-tagging. When presenting results for the interference we decided to include contributions of bottom quarks, setting bottom Yukawa coupling to zero, but we did check that the flavor-excitation topologies with b in the initial state change the results for (cq) channel by about three percent only.

(a) Higgs-boson transverse momentum.

(b) Higgs-boson rapidity.
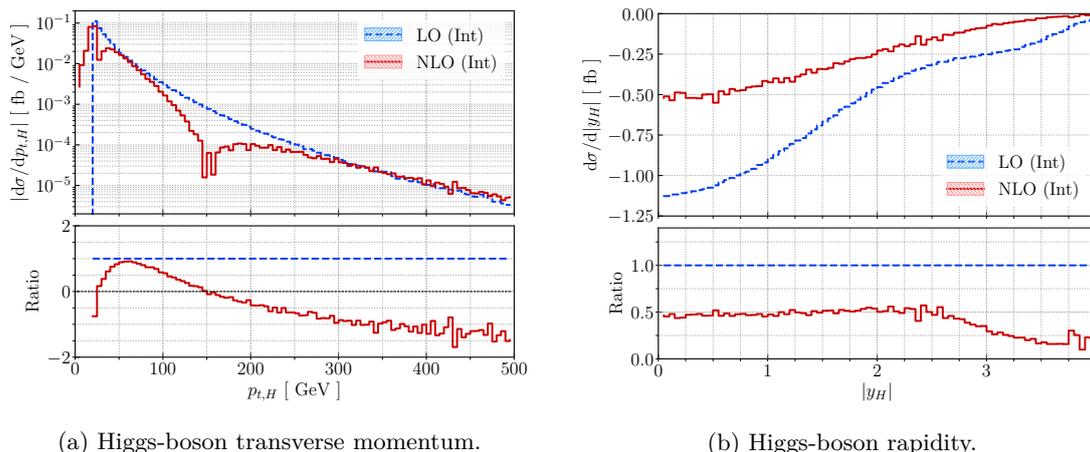
Figure 3. The transverse momentum and rapidity distributions of the Higgs boson calculated at LO (blue) and NLO (red) for central scale choice. We only consider the interference contribution. We note that the *absolute value* of $d\sigma_{\text{Int}}/dp_{t,H}$ is displayed in the left panel. This implies that this distribution actually changes sign at around $p_{t,H} \sim 150\,\text{GeV}$. The lower panels show ratios to the LO interference contribution.

real and virtual corrections in this case. Finally, we emphasize that it is unclear to what extent these various cancellations persist in higher orders; for this reason, a resummation of charm-mass logarithms for the interference contribution is desirable.

We continue with the discussion of kinematic distributions. We focus on the transverse momentum and the rapidity distributions of Higgs bosons in the interference contribution to $pp \to Hc$ cross section. They are shown in figure 3. We first discuss the transverse momentum distribution, figure 3a; when interpreting this figure it is important to recall that the *absolute* value of both LO and NLO distributions is plotted there and that the LO distribution is always *negative*. We observe in figure 3a that the leading-order distribution (blue) is large and negative at small $p_{t,H}$; as $p_{t,H}$ increases, the distribution goes to zero. The NLO QCD corrections affect the shape of the $p_{t,H}$ distribution. Indeed, a sharp edge at $p_{t,H} = 20\,\text{GeV}$, present at leading order, gets smeared at NLO. At moderate values of transverse momenta $p_{t,H} \sim 60\,\text{GeV}$ the K-factor is equal to one, while there is a large $\mathcal{O}(+50\%)$ reduction[11] at $p_{t,H} \sim 100\,\text{GeV}$. Second, at $p_{t,H} \sim 150\,\text{GeV}$ the NLO distribution goes through zero and becomes positive for larger values of $p_{t,H}$. Asymptotically, at even higher $p_{t,H}$ the LO and NLO distributions appear to be equal in absolute values but *opposite* in sign. Of course, all this happens at such high values of $p_{t,H}$ that are irrelevant for phenomenology, but it is quite a peculiar feature nevertheless.

Compared to Higgs transverse momentum distribution, the rapidity distribution of the Higgs boson in the interference contribution is much less volatile. Indeed, it follows from figure 3b that the difference between leading and next-to-leading-order distributions is well-described by a constant K-factor all the way up to $|y_H| \sim 2$. Beyond this value of the rapidity, the NLO distribution goes to zero faster than the LO one.

---

[11]"Reduction" in this case means that the distribution becomes less negative.

6 Conclusions

Production of Higgs bosons in association with charm jets at the LHC is mediated by two distinct mechanisms, one that involves the charm Yukawa coupling and the other one that involves an effective ggH vertex. Their interference involves a helicity flip and, for this reason, vanishes in the limit of massless charm quarks.

Since partonic cross sections are routinely computed for massless incoming partons and since the charm quark appears in the initial state in the main process $cg \to Hc$, it is interesting to understand how to circumvent the problem of having to deal with a massive parton in the initial state and to provide reliable estimate of the interference contribution.

We have addressed this problem by studying the $m_c \to 0$ limit of the helicity-flipping interference contribution including NLO QCD corrections. We have shown that the factorization of quasi-collinear and quasi-soft singularities in this case differs from the canonical pattern. We used explicit expressions for real and virtual matrix elements to extract logarithms of the charm quark mass and, having accomplished this, took the $m_c \to 0$ limit in the remaining parts of the computation. We removed parts of the $\mathcal{O}(\ln m_c)$ contributions by expressing results through conventional $\overline{\text{MS}}$ parton distribution functions valid for massless partons. Nevertheless, given an unconventional behavior of the interference in quasi-soft and quasi-collinear limits, logarithms of the charm quark mass survive in the final result for the NLO QCD corrections.

We have found that the absolute value of the leading-order interference is reduced by about fifty percent once NLO QCD corrections are accounted for. This significant but still "perturbatively acceptable" reduction is the result of a *very strong* cancellation between terms that involve double and single logarithms of the charm quark mass. We have observed that the NLO QCD corrections to the interference are kinematics-dependent and may change shapes of certain kinematic distributions in a significant way.

Higgs boson production in association with a charm jet is a promising way to study charm Yukawa coupling at the LHC [12]. The interference contribution, that is estimated to be about 10 percent of the Yukawa contribution at leading order, could have been perturbatively unstable given the required helicity flip and an unconventional pattern of quasi-soft and quasi-collinear limits. We addressed this question by performing a dedicated NLO QCD computation for the interference term and did not find a strong indication that this might be the case. Nevertheless, the moderate size of the NLO QCD corrections is the consequence of a very strong cancellations between double and single logarithms of the charm mass. It is unclear if this cancellation persists in higher orders. Hence, resummation of $\mathcal{O}(\ln m_c)$-enhanced terms for this process is quite desirable. It would be also interesting to compare our results with predictions for the interference computed in the three-flavor scheme that can be extracted from refs. [14–16]. We leave such a comparison to future work.

A Extraction of the $\mathcal{O}(\ln m_c)$-enhanced contributions in the real corrections

In this appendix we describe a procedure to extract $\mathcal{O}(\ln m_c)$ contributions to real emission corrections. They arise because of the quasi-singular behavior of real emission amplitudes in the soft or collinear limits involving charm quarks. The potential singularities in these limits are regulated by the charm mass leading to an appearance of $\mathcal{O}(\ln m_c)$-enhanced terms when integrated over relevant phase spaces. To extract logarithms of m_c, we subtract approximate expressions from exact matrix elements that make the difference integrable in the $m_c \to 0$ limit and integrate the subtraction terms over unresolved phase space to explicitly extract logarithms of m_c.

As an example, we consider the gluon-gluon partonic channel, i.e.

$$g(p_1) + g(p_2) \longrightarrow H(p_H) + c(p_3) + \bar{c}(p_4) \, , \tag{A.1}$$

and discuss the extraction of $\mathcal{O}(\ln m_c)$ terms in detail. This channel is suitable for such a discussion since, if the charm-quark mass is kept finite, it is free of soft and collinear divergences. Hence, all relevant contributions can be computed numerically for small but finite m_c, and used to validate formulas where logarithms of m_c have been extracted and $m_c \to 0$ limit has been taken where appropriate.

As we already mentioned in the main text, we use the nested soft-collinear subtraction scheme which, at this order, is equivalent to the FKS subtraction scheme [41, 42]. The details of the subtraction scheme can be found in the literature [37–40] and we do not repeat this discussion here. Nevertheless, the treatment of quasi-collinear and quasi-soft singularities related to the emission of *massive* charm quarks is new and requires an explanation.

We focus on the interference contribution between the Yukawa-like and the *ggH*-like production mechanisms in the process eq. (A.1). The interference term is non-zero only if helicity flip on the charm line occurs. Furthermore, the presence of such a helicity flip causes the usual factorization formulas to break down and the singular limits need to be explicitly analyzed. We note that, thanks to the symmetry of the squared amplitude for the process in eq. (A.1) under the exchange of c and $\bar{c}$, we can consider only the case where $\bar{c}$ quark becomes soft or quasi-collinear to one of the other partons. The case when both c and $\bar{c}$ become unresolved is impossible since we require a charm jet in the final state.

The quasi-singular limits which appear in this channel are related to the soft-quark limit S_4 with $E_4 \sim m_c$ and the three collinear limits C_{4i} with $i = 1, 2, 3$ where $(p_4 \cdot p_i) \sim m_c^2$. Performing an iterative subtraction of these singular limits, we find

$$\begin{aligned}
\langle F_{\mathrm{LM}}(1_g, 2_g; 3_c, 4_{\bar{c}}) \rangle = &\sum_{i=1}^{3} \langle (1 - C_{4i})(1 - S_4) \omega_{123}^{(i)} F_{\mathrm{LM}}(1_g, 2_g; 3_c, 4_{\bar{c}}) \rangle \\
&+ \langle C_{4i}(1 - S_4) \omega_{123}^{(i)} F_{\mathrm{LM}}(1_g, 2_g; 3_c, 4_{\bar{c}}) \rangle \\
&+ \langle S_4 F_{\mathrm{LM}}(1_g, 2_g; 3_c, 4_{\bar{c}}) \rangle \, ,
\end{aligned} \tag{A.2}$$

where the first term on the right-hand side denotes the fully-regulated contribution and the second and third terms are the collinear and the soft integrated subtraction terms. The

factors $\omega_{123}^{(i)}$ are the weights that describe various collinear sectors. They read

$$\omega_{123}^{(i)} = \frac{1}{\rho_{4i}} \cdot \left[\frac{1}{\rho_{41}} + \frac{1}{\rho_{42}} + \frac{1}{\rho_{43}} \right]^{-1}, \tag{A.3}$$

with $\rho_{4i} = 1 - \cos\theta_{4i}$. We note that, since all $m_c \to 0$ singularities are subtracted in the fully-regulated term in eq. (A.2), the $m_c \to 0$ limit can be immediately taken there. On the other hand, the integrated subtraction terms in the second line of eq. (A.2) require care to capture all the $\mathcal{O}(\ln m_c)$-terms and constants which survive the $m_c \to 0$ limit.

In the remaining part of this section, we discuss in detail the integration of the subtraction terms. We first focus on the soft subtraction term, i.e. the last term in eq. (A.2), and then the integration of the collinear subtraction term, i.e. the first term in the second line of eq. (A.2).

A.1 Integration of the soft-quark subtraction terms

Consider the soft-quark subtraction term

$$\langle S_4 F_{\mathrm{LM}}(1_g, 2_g; 3_c, 4_{\bar{c}}) \rangle. \tag{A.4}$$

To compute it, we need to know the behavior of the amplitude in the limit $p_4 \sim m_c \to 0$ and then integrate it over the phase space of the charm anti-quark with momentum p_4.

Although, normally, soft (gluon) emissions factorize into a product of an eikonal factor and a tree-level matrix element squared, a similar formula for soft-quark emission, relevant for helicity-flipping processes, does not exist. Hence, we determine the soft-quark limit of the interference by studying an explicit expression of the amplitude for the process in eq. (A.1) in the limit $p_4 \sim m_c \to 0$. We find

$$
\begin{aligned}
S_4 \mathrm{Int}\left[|\mathcal{M}(1_g, 2_g; 3_c, 4_{\bar{c}})|^2 \right] \sim\ & \frac{(2C_F - C_A)(p_1 \cdot p_2)}{(p_1 \cdot p_4)(p_2 \cdot p_4)} F_{12}(p_1, p_2, p_3) \\
& + \frac{C_A(p_1 \cdot p_3)}{(p_1 \cdot p_4)(m_c^2 + p_3 \cdot p_4)} F_{13}(p_1, p_2, p_3) \\
& + \frac{C_A(p_2 \cdot p_3)}{(p_2 \cdot p_4)(m_c^2 + p_3 \cdot p_4)} F_{23}(p_1, p_2, p_3),
\end{aligned}
\tag{A.5}
$$

where functions F_{ij} depend on the momenta p_1, p_2 and p_3 *only*. We emphasize that these functions are different from the leading-order interference contribution. The massless limit, $m_c \to 0$, can be now taken everywhere except for the eikonal factors and the phase-space measure of the unresolved parton $[\mathrm{d}p_4]$.

We write the integrated soft subtraction term as follows

$$
\begin{aligned}
\langle S_4 F_{\mathrm{LM}}(1_g, 2_g; 3_c, 4_{\bar{c}}) \rangle =\ & (2C_F - C_A) \langle F_{12}(p_1, p_2, p_3) \cdot \int \frac{[\mathrm{d}p_4](p_1 \cdot p_2)}{(p_1 \cdot p_4)(p_2 \cdot p_4)} \rangle \\
& + C_A \langle F_{13}(p_1, p_2, p_3) \cdot \int \frac{[\mathrm{d}p_4](p_1 \cdot p_3)}{(p_1 \cdot p_4)(m_c^2 + p_3 \cdot p_4)} \rangle \\
& + C_A \langle F_{23}(p_1, p_2, p_3) \cdot \int \frac{[\mathrm{d}p_4](p_2 \cdot p_3)}{(p_2 \cdot p_4)(m_c^2 + p_3 \cdot p_4)} \rangle,
\end{aligned}
\tag{A.6}
$$

where $\langle\ldots\rangle$ denotes the phase space integration and the relevant soft integrals can be found in appendix B. We stress that soft integrals are finite in four dimensions since they are naturally regulated by the charm-quark mass m_c.

A.2 Integration of the quasi-collinear subtraction terms

In this subsection, we discuss how to define and compute the soft-subtracted quasi-collinear limits of the interference contribution using the process in eq. (A.1) as an example. We focus on the sector 43 where c and $\bar{c}$ become collinear to each other. The relevant quantity reads[12]

$$\langle C_{43}(1 - S_4)F_{\mathrm{LM}}(1_g, 2_g; 3_c, 4_{\bar{c}})\rangle. \tag{A.7}$$

To proceed further, we split the above formula into collinear and soft-collinear terms

$$\langle C_{43}(1 - S_4)F_{\mathrm{LM}}(1_g, 2_g; 3_c, 4_{\bar{c}})\rangle = \langle C_{43}F_{\mathrm{LM}}(1_g, 2_g; 3_c, 4_{\bar{c}})\rangle - \langle C_{43}S_4 F_{\mathrm{LM}}(1_g, 2_g; 3_c, 4_{\bar{c}})\rangle. \tag{A.8}$$

We first discuss the collinear subtraction term $\langle C_{43}F_{\mathrm{LM}}(1_g, 2_g; 3_c, 4_{\bar{c}})\rangle$ defined as follows

$$\langle C_{43}F_{\mathrm{LM}}(1_g, 2_g; 3_c, 4_{\bar{c}})\rangle = \sum_{i=1}^{2} \int [\mathrm{d}p_H][\mathrm{d}p_3][\mathrm{d}p_4](2\pi)^4 \delta\left(p_{12} - p_H - p_3 - \bar{p}_4\right) \\ \times \frac{1}{(p_3 + p_4)^2} \frac{p_i \cdot p_3}{p_i \cdot \bar{p}_4} C_i(1_g, 2_g, 3_c, \bar{4}_{\bar{c}}). \tag{A.9}$$

In the above equation, the functions $C_{1,2}$ depend on the momenta p_1, p_2, p_3 and $\bar{p}_4$. The bar over momentum p_4 indicates that the relevant collinear limit has been taken, i.e.

$$C_{43}p_4 = (E_4, \beta_4 \vec{n}_3) \equiv \bar{p}_4. \tag{A.10}$$

Note that in eq. (A.10) $\beta_4 = \sqrt{1 - m_c^2/E_4^2}$ is the velocity of $\bar{c}$ and $\vec{n}_3$ is a unit vector pointing in the direction of momentum $\vec{p}_3$. We note that in eq. (A.9) the massless limit $m_c \to 0$ has not been taken. We also note that the functions $C_{1,2}$ are regular in the soft-quark limit, $E_4 \to m_c \sim 0$.

Our goal is to extract all $\mathcal{O}(\ln m_c)$ terms arising from eq. (A.9) and take the massless limit after that. To do so, we add and subtract the soft limits of the functions C_i

$$C_i(1_g, 2_g, 3_c, \bar{4}_{\bar{c}}) = \left[C_i(1_g, 2_g, 3_c, \bar{4}_{\bar{c}}) - C_{i,\mathrm{soft}}(1_c, 2_g, 3_c)\right] + C_{i,\mathrm{soft}}(1_c, 2_g, 3_c), \tag{A.11}$$

where $C_{i,\mathrm{soft}}(1_c, 2_g, 3_c) = C_i(1_g, 2_g, 3_c, 0)$. The above procedure splits the integral in eq. (A.9) into two parts: the *regulated* integral that contains the expression in the square bracket in eq. (A.11) and the *soft* part. In the regulated part, the soft divergence at $E_4 = 0$ has been regularized. This implies that, after integrating $1/(p_3 + p_4)^2$ over the relative angle between p_3 and p_4 and extracting logarithms of m_c from this angular integral, we can

---

[12]We note that weight factors introduced in eq. (A.3) do not appear in the collinear limits.

set m_c to zero everywhere else right away. We obtain

$$\langle C_{43} F_{\mathrm{LM}}(1_g, 2_g; 3_c, 4_{\bar{c}}) \rangle_{\mathrm{reg}} = \frac{1}{(2\pi)^2} \sum_{i=1}^{2} \int [\mathrm{d}p_H][\mathrm{d}p_3](2\pi)^4 \delta\left(p_{12} - p_H - p_{34}\right)$$

$$\int_0^1 \frac{z\,\mathrm{d}z}{1-z} \Big[C_i(1_g, 2_g, z34, (1-z)34) - C_{i,\mathrm{soft}}(1_c, 2_g, z34) \Big]$$

$$\times \Big[\ln(2E_{34}/m_c) + \ln(1-z) + \ln(z) \Big], \tag{A.12}$$

where we have used the fact that in $m_c \to 0$ limit we can write $p_3 = zp_{34}$ and $\bar{p}_4 = (1-z)p_{34}$ for $p_{34}^2 = 0$.

We will now discuss the soft part of the collinear subtraction term. It reads

$$\langle C_{43} F_{\mathrm{LM}}(1_g, 2_g; 3_c, 4_{\bar{c}}) \rangle_{\mathrm{soft}} = \sum_{i=1}^{2} \int [\mathrm{d}p_H][\mathrm{d}p_3][\mathrm{d}p_4](2\pi)^4 \delta\left(p_{12} - p_H - p_3 - \bar{p}_4\right)$$

$$\times \frac{1}{(p_3 + p_4)^2} \frac{p_i \cdot p_3}{p_i \cdot \bar{p}_4} C_{i,\mathrm{soft}}(1_c, 2_g, 3_c). \tag{A.13}$$

We emphasize that this term still contains soft singularity and, for this reason, the $m_c \to 0$ limit cannot be taken. However, it is convenient to combine this integral with the soft-collinear subtraction term $\langle C_{43} S_4 F_{\mathrm{LM}}(1_g, 2_g; 3_c, 4_{\bar{c}}) \rangle$, cf. eq. (A.8); if this is done, the required computations simplify significantly.

The soft-collinear integrated subtraction term in sector 43 reads

$$\langle C_{43} S_4 F_{\mathrm{LM}}(1_g, 2_g; 3_c, 4_{\bar{c}}) \rangle = \sum_{i=1}^{2} \int [\mathrm{d}p_H][\mathrm{d}p_3][\mathrm{d}p_4](2\pi)^4 \delta\left(p_{12} - p_H - p_3\right)$$

$$\times \frac{2C_A F_{i3}(p_1, p_2, p_3)}{(p_3 + p_4)^2} \frac{p_i \cdot p_3}{p_i \cdot \bar{p}_4}. \tag{A.14}$$

To derive this result we used the soft-limit of the interference amplitude reported in eq. (A.5). We emphasize that, since the soft operator is present on the left hand side in the above equation, the soft-quark momentum p_4 is removed from the energy-momentum conserving delta-function. Moreover, since

$$C_{i,\mathrm{soft}}(1_c, 2_g, 3_c) = 2C_A F_{i3}(p_1, p_2, p_3), \tag{A.15}$$

the two integrals in eqs. (A.13), (A.14) appear to be the same up to the argument of the delta-functions. We combine the two integrals and find

$$\langle C_{43} F_{\mathrm{LM}}(1_g, 2_g; 3_c, 4_{\bar{c}}) \rangle_{\mathrm{soft}} - \langle C_{43} S_4 F_{\mathrm{LM}}(1_g, 2_g; 3_c, 4_{\bar{c}}) \rangle =$$

$$= \sum_{i=1}^{2} \int [\mathrm{d}p_H][\mathrm{d}p_3][\mathrm{d}p_4](2\pi)^4 \Big[\delta\left(p_{12} - p_H - p_3 - \bar{p}_4\right) - \delta\left(p_{12} - p_H - p_3\right) \Big]$$

$$\times \frac{2C_A F_{i3}(p_1, p_2, p_3)}{(p_3 + p_4)^2} \frac{p_i \cdot p_3}{p_i \cdot \bar{p}_4}. \tag{A.16}$$

To proceed further, we note that it is straightforward to integrate over directions of the quark with momentum p_4 but integration over its energy is more involved. It is convenient to split the E_4 integration into two regions by introducing an auxiliary parameter σ

$$1 = \Theta(E_4 - \sigma) + \Theta(\sigma - E_4). \tag{A.17}$$

We choose σ to satisfy the following inequality $m_c \ll \sigma \ll E_3$. For small energies, $E_4 < \sigma \ll E_3$, we can drop the momentum $\bar{p}_4$ from the energy momentum conserving delta-function which leads to

$$\left[\delta\left(p_{12} - p_H - p_3 - \bar{p}_4\right) \left[\Theta(E_4 - \sigma) + \Theta(\sigma - E_4)\right] - \delta\left(p_{12} - p_H - p_3\right) \right] =$$
$$= \left[\delta\left(p_{12} - p_H - p_3 - \bar{p}_4\right) - \delta\left(p_{12} - p_H - p_3\right) \right] \Theta(E_4 - \sigma) + \mathcal{O}(\sigma/E_3). \tag{A.18}$$

This relation implies that the integrand in eq. (A.16) is non-vanishing only in the high-energy domain where $E_4 > \sigma \gg m_c$ and, therefore, the limit $m_c \to 0$ can be taken. This leads to the following expression

$$\langle C_{43} F_{\mathrm{LM}}(1_g, 2_g; 3_c, 4_{\bar{c}}) \rangle_{\mathrm{soft}} - \langle C_{43} S_4 F_{\mathrm{LM}}(1_g, 2_g; 3_c, 4_{\bar{c}}) \rangle =$$

$$= \frac{C_A}{(2\pi)^2} \sum_{i=1}^{2} \int [\mathrm{d}p_H][\mathrm{d}p_{34}](2\pi)^4 \delta(p_{12} - p_H - p_{34})$$

$$\left\{ \int_{z_{\min}}^{z_{\max}} \frac{\mathrm{d}z}{1-z} \ln\left(\frac{2E_{34}(1-z)z}{m_c}\right) \left[z\theta(z)F_{i3}(p_1, p_2, zp_{34}) - F_{i3}(p_1, p_2, p_{34}) \right] \right.$$

$$\left. + \int_{z_{\min}}^{z_{\max}} \frac{\mathrm{d}z}{1-z} \ln\left((2-z)z\right) F_{i3}(p_1, p_2, p_{34}) \right\}. \tag{A.19}$$

To arrive at eq. (A.19) we introduced the four-momentum $p_{34} = p_3 + \bar{p}_4$ and a variable z such that $p_3 = zp_{34}$ in terms that contain the delta-function $\delta(p_{12} - p_H - p_3 - \bar{p}_4)$. In terms that contain the delta-function $\delta(p_{12} - p_H - p_3)$, we set $(1-z) = E_4/E_3$, rename p_3 into p_{34} and set $\sigma \to 0$. The lower integration boundary $z_{\min}$ is given by $z_{\min} = 1 - E_{\max}/E_{34} < 0$.

In total, the integrated collinear term $\langle C_{43}(1 - S_4)F_{\mathrm{LM}}(1_g, 2_g; 3_c, 4_{\bar{c}}) \rangle$ is given by a sum of expressions in eqs. (A.12), (A.19). We describe a numerical check of validity of this result in the following section.

A.3 Numerical checks

Since the cross section of the gluon-gluon channel, eq. (A.1), is finite as long as we keep the non-zero charm mass, analytical results derived in the previous section can be checked numerically by computing $\sigma_{gg \to Hc\bar{c}}$ explicitly for small values of the charm mass without any approximation.

The comparison is shown in figure 4. We use fiducial cuts described in the main text and compare hadronic contributions to the interference for gg partonic channel computed in two different ways. Green points (rectangles) show the results of the computation without any approximation, i.e. by directly integrating the matrix element squared. Blue points
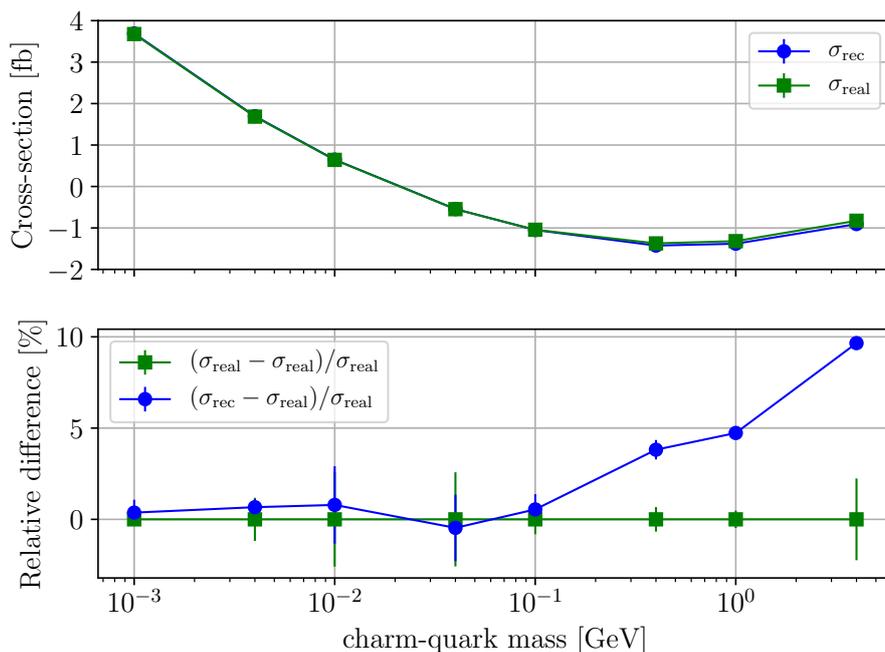
Figure 4. The cross section of the $gg \to Hc\bar{c}$ process calculated by a direct integration of the matrix element with non-zero charm-quark mass, σ_{real} (green rectangles), and reconstructed using procedure described in previous subsections, σ_{rec} (blue circles). We employ the same parameters and kinematic constraints as in the main text.

(circles) show the results of the computation that relies on the expansion around $m_c \to 0$ limit, as described in previous subsections. The two results should agree for small values of m_c. The upper panel of figure 4 shows the absolute values of the interference cross section in the gg partonic channel obtained with the two methods, while their difference is shown in the lower panel. We see a better and better agreement between the two results as we mover to smaller and smaller values of the charm-quark mass. This indicates that the m_c-dependence of the interference contribution is properly reconstructed.

B Soft-quark integrals

In this section we list integrals that are required for the integrated soft-quark subtraction terms. We need a number of integrals depending on the type and configuration of the emitters p_a and p_b as well as the propagator appearing in the eikonal factor.

We note that we are interested only in the terms that contain logarithms of the charm-quark mass and constant terms, but we drop all power-suppressed terms which vanish in the $m_c \to 0$ limit. All integrals are computed in $d = 4$ dimensions since all singularities are naturally regulated by the charm-quark mass.

The phase-space measure for a massive-quark emission, $p_4^2 = m_c^2$, reads

$$[\mathrm{d}p_4] = \frac{k_4^2 \mathrm{d}k_4}{2E_4} \frac{\mathrm{d}\Omega^{(3)}}{(2\pi)^3} \Theta(E_{\text{max}} - E_4)\Theta(E_4 - m_c) \,, \tag{B.1}$$

where k_4 is the length of $\vec{p}_4$ momentum, $\mathrm{d}\Omega^{(3)}$ denotes angular integration and $E_{\max}$ is the usual energy cutoff of the nested soft-collinear subtraction scheme. In the remaining part of this section, we list soft-quark integrals that are needed to obtain integrated soft-quark subtraction terms, see section A.1 for details.[13]

Two massless emitters: two emitters a, b have four-momenta $p_a = E_a(1, \vec{n}_a)$ and $p_b = E_b(1, \vec{n}_b)$, respectively. Both four-momenta are light-like $p_a^2 = p_b^2 = 0$. Vectors $\vec{n}_a$ and $\vec{n}_b$ describe direction of flight of the emitters; we refer to the opening angle between $\vec{n}_a$ and $\vec{n}_b$ as θ_{ab}.

The soft integral reads

$$\int \frac{[\mathrm{d}p_4](p_a \cdot p_b)}{(p_a \cdot p_4)(p_b \cdot p_4)} = \frac{1}{(2\pi)^2}\left[\ln^2(2s_{ab}E_{\max}/m_c) - \frac{\pi^2}{12} + \frac{1}{2}\mathrm{Li}_2(c_{ab}^2)\right], \tag{B.2}$$

where we used $s_{ab} = \sin(\theta_{ab}/2)$ and $c_{ab} = \cos(\theta_{ab}/2)$.

One massive and one massless emitters: two emitters a, b have four-momenta $p_a = E_a(1, \vec{n}_a)$ and $p_b = E_b(1, \beta_b \vec{n}_b)$, respectively. They satisfy $p_a^2 = 0$ and $p_b^2 = m_c^2$. We refer to the opening angle between $\vec{n}_a$ and $\vec{n}_b$ as θ_{ab}. We require three soft integrals of this type

$$\begin{aligned}
\int \frac{[\mathrm{d}p_4](p_a \cdot p_b)}{(p_a \cdot p_4)(m_c^2 + p_b \cdot p_4)} &= \frac{1}{(2\pi)^2}\left[\ln^2(2s_{ab}E_{\max}/m_c) - \frac{\pi^2}{12}\right.\\
&\quad \left. + \mathrm{Li}_2(-E_{\max}/E_b) + \frac{1}{2}\mathrm{Li}_2(c_{ab}^2)\right],\\[4pt]
\int \frac{[\mathrm{d}p_4](p_a \cdot p_b)}{(p_a \cdot p_4)(p_b \cdot p_4)} &= \frac{1}{(2\pi)^2}\left[\ln^2(2s_{ab}E_{\max}/m_c) + \frac{1}{4}\mathrm{Li}_2(-E_{\max}^2/E_b^2)\right.\\
&\quad \left. - \frac{\pi^2}{12} + \frac{1}{2}\mathrm{Li}_2(c_{ab}^2)\right],\\[4pt]
\int \frac{[\mathrm{d}p_4](p_a \cdot p_b)}{(p_a \cdot p_4)(m_c^2 - p_b \cdot p_4)} &= \frac{1}{(2\pi)^2}\left[-\ln^2(2s_{ab}E_{\max}/m_c) + \mathrm{Li}_2(1 - E_{\max}/E_b)\right.\\
&\quad \left. - \frac{1}{2}\mathrm{Li}_2(c_{ab}^2) + \ln(E_{\max}/E_b)\ln(E_{\max}/E_b - 1) - \frac{\pi^2}{12}\right],
\end{aligned} \tag{B.3}$$

where we used $s_{ab} = \sin(\theta_{ab}/2)$ and $c_{ab} = \cos(\theta_{ab}/2)$.

Two massive emitters: two emitters a, b have four-momenta $p_a = E_a(1, \beta_a \vec{n}_a)$ and $p_b = E_b(1, \beta_b \vec{n}_b)$, respectively. They satisfy $p_a^2 = p_b^2 = m_c^2$. We refer to the opening angle

---

[13]Similar expressions to those in section A.1 can be derived for other partonic channels featuring soft-quark singularities, i.e. cc and $c\bar{c}$.

between $\vec{n}_a$ and $\vec{n}_b$ as θ_{ab}. In this case, we use $E_{\max} = E_a$. We find

$$\int \frac{[\mathrm{d}p_4](p_a \cdot p_b)}{(m_c^2 - p_a \cdot p_4)(m_c^2 + p_b \cdot p_4)} = \frac{1}{(2\pi)^2} \left[-\ln^2(2s_{ab}E_{\max}/m_c) - \frac{\pi^2}{12} \right.$$
$$\left. - \frac{1}{2}\mathrm{Li}_2(c_{ab}^2) - \mathrm{Li}_2(-E_{\max}/E_b) \right], \qquad \text{(B.4)}$$

$$\int \frac{[\mathrm{d}p_4](p_a \cdot p_b)}{(m_c^2 - p_a \cdot p_4)(m_c^2 - p_b \cdot p_4)} = \frac{1}{(2\pi)^2} \left[\ln^2(2E_{\max}/m_c) + \frac{\pi^2}{4} \right],$$

where we used $s_{ab} = \sin(\theta_{ab}/2)$ and $c_{ab} = \cos(\theta_{ab}/2)$.

Open Access. This article is distributed under the terms of the Creative Commons Attribution License ([CC-BY 4.0](#)), which permits any use, distribution and reproduction in any medium, provided the original author(s) and source are credited.

References

[1] ATLAS collaboration, *Observation of $H \to b\bar{b}$ decays and VH production with the ATLAS detector*, *Phys. Lett. B* **786** (2018) 59 [arXiv:1808.08238] [INSPIRE].

[2] CMS collaboration, *Observation of Higgs boson decay to bottom quarks*, *Phys. Rev. Lett.* **121** (2018) 121801 [arXiv:1808.08242] [INSPIRE].

[3] ATLAS collaboration, *Cross-section measurements of the Higgs boson decaying into a pair of τ-leptons in proton-proton collisions at $\sqrt{s} = 13$ TeV with the ATLAS detector*, *Phys. Rev. D* **99** (2019) 072001 [arXiv:1811.08856] [INSPIRE].

[4] CMS collaboration, *Search for the associated production of the Higgs boson and a vector boson in proton-proton collisions at $\sqrt{s} = 13$ TeV via Higgs boson decays to τ leptons*, *JHEP* **06** (2019) 093 [arXiv:1809.03590] [INSPIRE].

[5] ATLAS collaboration, *A search for the dimuon decay of the Standard Model Higgs boson with the ATLAS detector*, *Phys. Lett. B* **812** (2021) 135980 [arXiv:2007.07830] [INSPIRE].

[6] CMS collaboration, *Search for the Higgs boson decaying to two muons in proton-proton collisions at $\sqrt{s} = 13$ TeV*, *Phys. Rev. Lett.* **122** (2019) 021801 [arXiv:1807.06325] [INSPIRE].

[7] G. Perez, Y. Soreq, E. Stamou and K. Tobioka, *Prospects for measuring the Higgs boson coupling to light quarks*, *Phys. Rev. D* **93** (2016) 013001 [arXiv:1505.06689] [INSPIRE].

[8] A.L. Kagan, G. Perez, F. Petriello, Y. Soreq, S. Stoynev and J. Zupan, *Exclusive Window onto Higgs Yukawa Couplings*, *Phys. Rev. Lett.* **114** (2015) 101802 [arXiv:1406.1722] [INSPIRE].

[9] T. Modak and R. Srivastava, *Probing anomalous Higgs couplings in $H \to ZV$ decays*, *Mod. Phys. Lett. A* **32** (2017) 1750004 [arXiv:1411.2210] [INSPIRE].

[10] M. König and M. Neubert, *Exclusive Radiative Higgs Decays as Probes of Light-Quark Yukawa Couplings*, *JHEP* **08** (2015) 012 [arXiv:1505.03870] [INSPIRE].

[11] F. Bishara, U. Haisch, P.F. Monni and E. Re, *Constraining Light-Quark Yukawa Couplings from Higgs Distributions*, *Phys. Rev. Lett.* **118** (2017) 121801 [arXiv:1606.09253] [INSPIRE].

[12] I. Brivio, F. Goertz and G. Isidori, *Probing the Charm Quark Yukawa Coupling in Higgs + Charm Production*, *Phys. Rev. Lett.* **115** (2015) 211801 [`arXiv:1507.02916`] [INSPIRE].

[13] N.M. Coyle, C.E.M. Wagner and V. Wei, *Bounding the charm Yukawa coupling*, *Phys. Rev. D* **100** (2019) 073013 [`arXiv:1905.09360`] [INSPIRE].

[14] S. Dittmaier, M. Krämer and M. Spira, *Higgs radiation off bottom quarks at the Tevatron and the CERN LHC*, *Phys. Rev. D* **70** (2004) 074010 [`hep-ph/0309204`] [INSPIRE].

[15] S. Dawson, C.B. Jackson, L. Reina and D. Wackeroth, *Exclusive Higgs boson production with bottom quarks at hadron colliders*, *Phys. Rev. D* **69** (2004) 074027 [`hep-ph/0311067`] [INSPIRE].

[16] S. Dawson, C.B. Jackson, L. Reina and D. Wackeroth, *Higgs boson production with one bottom quark jet at hadron colliders*, *Phys. Rev. Lett.* **94** (2005) 031802 [`hep-ph/0408077`] [INSPIRE].

[17] A.A. Penin, *High-Energy Limit of Quantum Electrodynamics beyond Sudakov Approximation*, *Phys. Lett. B* **745** (2015) 69 [*Erratum ibid.* **751** (2015) 596] [*Erratum ibid.* **771** (2017) 633] [`arXiv:1412.0671`] [INSPIRE].

[18] K. Melnikov and A. Penin, *On the light quark mass effects in Higgs boson production in gluon fusion*, *JHEP* **05** (2016) 172 [`arXiv:1602.09020`] [INSPIRE].

[19] Z.L. Liu and M. Neubert, *Factorization at subleading power and endpoint-divergent convolutions in $h \to \gamma\gamma$ decay*, *JHEP* **04** (2020) 033 [`arXiv:1912.08818`] [INSPIRE].

[20] Z.L. Liu, B. Mecaj, M. Neubert and X. Wang, *Factorization at subleading power and endpoint divergences in $h \to \gamma\gamma$ decay. Part II. Renormalization and scale evolution*, *JHEP* **01** (2021) 077 [`arXiv:2009.06779`] [INSPIRE].

[21] E. Laenen, J. Sinninghe Damsté, L. Vernazza, W. Waalewijn and L. Zoppi, *Towards all-order factorization of QED amplitudes at next-to-leading power*, *Phys. Rev. D* **103** (2021) 034022 [`arXiv:2008.01736`] [INSPIRE].

[22] S. Catani, S. Dittmaier and Z. Trócsányi, *One loop singular behavior of QCD and SUSY QCD amplitudes with massive partons*, *Phys. Lett. B* **500** (2001) 149 [`hep-ph/0011222`] [INSPIRE].

[23] R. Doria, J. Frenkel and J.C. Taylor, *Counter Example to NonAbelian Bloch-Nordsieck Theorem*, *Nucl. Phys. B* **168** (1980) 93 [INSPIRE].

[24] C. Di'Lieto, S. Gendron, I.G. Halliday and C.T. Sachrajda, *A Counter Example to the Bloch-Nordsieck Theorem in NonAbelian Gauge Theories*, *Nucl. Phys. B* **183** (1981) 223 [INSPIRE].

[25] J. Frenkel, J.G.M. Gatheral and J.C. Taylor, *Quark-antiquark annihilation is infrared safe at high-energy to all orders*, *Nucl. Phys. B* **233** (1984) 307 [INSPIRE].

[26] S. Catani, M. Ciafaloni and G. Marchesini, *Noncancelling infrared divergences in QCD coherent state*, *Nucl. Phys. B* **264** (1986) 588 [INSPIRE].

[27] S. Catani, *Violation of the Bloch-Nordsieck Mechanism in General NonAbelian Theories and SUSY QCD*, *Z. Phys. C* **37** (1988) 357 [INSPIRE].

[28] A. Andrasi, M. Day, R. Doria, J. Frenkel and J.C. Taylor, *Soft Divergences in Perturbative QCD*, *Nucl. Phys. B* **182** (1981) 104 [INSPIRE].

[29] C.A. Nelson, *Avoidance of counter-example to non-Abelian Bloch-Nordsieck conjecture by using coherent state approach*, *Nucl. Phys. B* **186** (1981) 187.

[30] I. Ito, *Cancellation of Infrared Divergence and Initial Degenerate State in QCD*, *Prog. Theor. Phys.* **65** (1981) 1466 [INSPIRE].

[31] N. Yoshida, *Diagrammatical Display of the Counter Example to NonAbelian Bloch-Nordsieck Conjecture*, *Prog. Theor. Phys.* **66** (1981) 269 [INSPIRE].

[32] N. Yoshida, *Cancellation of the infrared singularity through the unitarity relation*, *Prog. Theor. Phys.* **66** (1981) 1803 [INSPIRE].

[33] T. Muta and C.A. Nelson, *Role of Quark-Gluon Degenerate States in Perturbative QCD*, *Phys. Rev. D* **25** (1982) 2222 [INSPIRE].

[34] B.F.L. Ward, *Quark masses and resummation in precision QCD theory*, *Phys. Rev. D* **78** (2008) 056001 [arXiv:0707.2101] [INSPIRE].

[35] F. Caola, K. Melnikov, D. Napoletano and L. Tancredi, *Noncancellation of infrared singularities in collisions of massive quarks*, *Phys. Rev. D* **103** (2021) 054013 [arXiv:2011.04701] [INSPIRE].

[36] S. Frixione, *Initial conditions for electron and photon structure and fragmentation functions*, *JHEP* **11** (2019) 158 [arXiv:1909.03886] [INSPIRE].

[37] F. Caola, K. Melnikov and R. Röntsch, *Nested soft-collinear subtractions in NNLO QCD computations*, *Eur. Phys. J. C* **77** (2017) 248 [arXiv:1702.01352] [INSPIRE].

[38] F. Caola, K. Melnikov and R. Röntsch, *Analytic results for color-singlet production at NNLO QCD with the nested soft-collinear subtraction scheme*, *Eur. Phys. J. C* **79** (2019) 386 [arXiv:1902.02081] [INSPIRE].

[39] F. Caola, K. Melnikov and R. Röntsch, *Analytic results for decays of color singlets to gg and $q\bar{q}$ final states at NNLO QCD with the nested soft-collinear subtraction scheme*, *Eur. Phys. J. C* **79** (2019) 1013 [arXiv:1907.05398] [INSPIRE].

[40] K. Asteriadis, F. Caola, K. Melnikov and R. Röntsch, *Analytic results for deep-inelastic scattering at NNLO QCD with the nested soft-collinear subtraction scheme*, *Eur. Phys. J. C* **80** (2020) 8 [arXiv:1910.13761] [INSPIRE].

[41] S. Frixione, Z. Kunszt and A. Signer, *Three jet cross-sections to next-to-leading order*, *Nucl. Phys. B* **467** (1996) 399 [hep-ph/9512328] [INSPIRE].

[42] S. Frixione, *A General approach to jet cross-sections in QCD*, *Nucl. Phys. B* **507** (1997) 295 [hep-ph/9706545] [INSPIRE].

[43] A. Behring and W. Bizoń, *Higgs decay into massive b-quarks at NNLO QCD in the nested soft-collinear subtraction scheme*, *JHEP* **01** (2020) 189 [arXiv:1911.11524] [INSPIRE].

[44] S. Catani and M.H. Seymour, *A General algorithm for calculating jet cross-sections in NLO QCD*, *Nucl. Phys. B* **485** (1997) 291 [*Erratum ibid.* **510** (1998) 503] [hep-ph/9605323] [INSPIRE].

[45] G. Passarino and M.J.G. Veltman, *One Loop Corrections for e^+e^- Annihilation Into $\mu^+\mu^-$ in the Weinberg Model*, *Nucl. Phys. B* **160** (1979) 151 [INSPIRE].

[46] R. Mondini, U. Schubert and C. Williams, *Top-induced contributions to $H \to b\bar{b}$ and $H \to c\bar{c}$ at $\mathcal{O}(\alpha_s^3)$*, *JHEP* **12** (2020) 058 [arXiv:2006.03563] [INSPIRE].

[47] S. Catani, *The Singular behavior of QCD amplitudes at two loop order*, *Phys. Lett. B* **427** (1998) 161 [hep-ph/9802439] [INSPIRE].

[48] R. Mertig, M. Böhm and A. Denner, *FEYN CALC: Computer algebraic calculation of Feynman amplitudes*, *Comput. Phys. Commun.* **64** (1991) 345 [INSPIRE].

[49] V. Shtabovenko, R. Mertig and F. Orellana, *FeynCalc 9.3: New features and improvements*, *Comput. Phys. Commun.* **256** (2020) 107478 [arXiv:2001.04407] [INSPIRE].

[50] H.H. Patel, *Package-X: A Mathematica package for the analytic calculation of one-loop integrals*, *Comput. Phys. Commun.* **197** (2015) 276 [arXiv:1503.01469] [INSPIRE].

[51] A. Buckley et al., *LHAPDF6: parton density access in the LHC precision era*, *Eur. Phys. J. C* **75** (2015) 132 [arXiv:1412.7420] [INSPIRE].

[52] NNPDF collaboration, *Parton distributions from high-precision collider data*, *Eur. Phys. J. C* **77** (2017) 663 [arXiv:1706.00428] [INSPIRE].

[53] K.G. Chetyrkin, J.H. Kühn and M. Steinhauser, *RunDec: A Mathematica package for running and decoupling of the strong coupling and quark masses*, *Comput. Phys. Commun.* **133** (2000) 43 [hep-ph/0004189] [INSPIRE].

[54] F. Herren and M. Steinhauser, *Version 3 of RunDec and CRunDec*, *Comput. Phys. Commun.* **224** (2018) 333 [arXiv:1703.03751] [INSPIRE].